Journal of Cellular Biochemistry 94:669–683 (2005)

Formation of a Physiological Complex Between TRPV2 and RGA Protein Promotes Cell Surface Expression of TRPV2

Alexander J. Stokes,[1] Clay Wakano,[1] Kimberly A. del Carmen,[1] Murielle Koblan-Huberson,[1] and Helen Turner[1,2]*

[1]Laboratory of Cell Biology and Immunology, Center for Biomedical Research at the Queen's Medical Center, Honolulu, Hawaii
[2]Department of Cell and Molecular Biology, John A. Burns School of Medicine, University of Hawaii, Hawaii

Abstract The transient receptor potential, sub-family Vanilloid $(TRPV)_2$ cation channel is activated in response to extreme temperature elevations in sensory neurons. However, TRPV2 is widely expressed in tissues with no sensory function, including cells of the immune system. Regulation of GRC, the murine homolog of TRPV2 has been studied in insulinoma cells and myocytes. GRC is activated in response to certain growth factors and neuropeptides, via a mechanism that involves regulated access of the channel to the plasma membrane. This is likely to be an important primary control mechanism for TRPV2 outside the CNS. Here, we report that a regulated trafficking step controls the access of TRPV2 to the cell surface in mast cells. In mast cells, elevations in cytosolic cAMP are sufficient to drive plasma membrane localization of TRPV2. We have previously proposed that the recombinase gene activator protein (RGA), a four-transmembrane domain, intracellular protein, associates with TRPV2 during the biosynthesis and early trafficking of the channel. We use a polyclonal antibody to RGA to confirm the formation of a physiological complex between RGA and TRPV2. Finally, we show that over-expression of the RGA protein potentiates the basal surface localization of TRPV2. We propose that trafficking and activation mechanisms intersect for TRPV2, and that cAMP mobilizing stimuli may regulate TRPV2 localization in non-sensory cells. RGA participates in the control of TRPV2 surface levels, and co-expression of RGA may be a key component of experimental systems that seek to study TRPV2 physiology. J. Cell. Biochem. 94: 669–683, 2005.

Key words: ion channels; trafficking; TRPV2; mast cells

Various classes of ion channel are regulated by protein–protein interactions at a level that precedes their association with signaling complexes at the plasma membrane. Many channels are hetero-oligomers, with the pore-forming units associated with non-pore-forming accessory subunits [Green and Millar, 1995; MacKrill, 1999; Deutsch, 2002; Trimmer, 2002]. Accessory subunits often associate intracellularly with the channel proteins and accompany them to the cell surface. Diverse roles have been documented for these accessory proteins, including regulation of trafficking to the cell surface and interaction with regulatory second messengers or proteins that modulate channel gating or kinetics. During the early stages of biosynthesis and trafficking, channels undergo complex processing [Chang et al., 1997; Gothel and Marahiel, 1999; Deutsch, 2002]. Channel biogenesis may include post-translational modification such as multi-stage glycosylation, directed proteolysis, and lipidation [Green and Millar, 1995; Petrecca et al., 1999; Kedei et al., 2001]. Moreover, channels must maintain a complex topology, and oligomerization of the pore-forming units must proceed with an accuracy that guarantees absolute alignment of the

Grant sponsor: Charles E. Culpeper Biomedical Pilot initiative (Rockefeller Brothers Fund) (to HT); Grant sponsor: National Institute of General Medical Sciences (to HT); Grant number: RO1 GM70634-01.

*Correspondence to: Helen Turner, PhD, Queen's Center for Biomedical Research, 1301 Punchbowl Street, University Tower 811, Honolulu, Hawaii, 96813.
E-mail: hturner@queens.org

Received 4 June 2004; Accepted 8 September 2004
DOI 10.1002/jcb.20331

selectivity filter region. Endoplasmic reticulum- and Golgi-resident accessory proteins assist in directing and maintaining the integrity of these processes.

Cation channels of the transient receptor potential, sub-family Vanilloid (TRPV) family respond to diverse stimuli, and can confer the ability to sense changes in the physical environment upon cells in which they are expressed [Clapham, 2002; Minke and Cook, 2002; Benham et al., 2003]. TRPV2 has been described as a heat-activated channel [Caterina and Julius, 1999, 2001]. In sensory neurons and in heterologus expression systems, exposure to temperatures $>52^{\circ}C$ has been shown to specifically induce TRPV2 activity. TRPV2 is therefore a component of the physiological response to noxious thermal stimuli [Caterina et al., 1999; Clapham, 2002; Minke and Cook, 2002]. However, sensory neurons are not the sole location for TRPV2. Several reports place TRPV2 at the mRNA and protein level in cell types that lack sensory function, including myocytes, neutrophils, hepatoblastoma, and insulinoma cells [Kanzaki et al., 1999; Boels et al., 2001; Heiner et al., 2003a,b; Muraki et al., 2003]. Interestingly, TRPV2 mRNA is widely expressed within cells of the immune system, and we have previously shown that TRPV2 is present and functional in mast cells [Bradding and Conley, 2002; Barnhill et al., 2004; Stokes et al., 2004]. Expression of TRPV2 in non-sensory tissues creates a necessity for the identification of an activation mechanism specific to these cell types.

A murine TRPV2 homolog, the GRC channel, displays regulated trafficking to the cell surface following growth factor stimulation of insulinoma cells [Kanzaki et al., 1999], and a similar activation pathway has been documented in response to a neuropeptide in neuroendocrine cells [Boels et al., 2001]. Both stimuli result in appearance of an active conductance at the cell surface. Thus for GRC, it appears that trafficking and activation mechanisms intersect. In the present report, we describe that a regulated trafficking step enhances surface expression of TRPV2 in mast cells. In this cell system, a cAMP-mobilizing stimulus is sufficient to induce surface expression of TRPV2. We have proposed that elucidation of the protein–protein interactions that are made by TRPV2 may provide insight into possible regulatory mechanisms, including components of both trafficking and acute activation pathways. We have previously identified that an interaction between TRPV2 and recombinase gene activator (RGA) [Tagoh et al., 1996], a four-transmembrane domain protein with no previously assigned function, takes place intracellularly in a cellular over-expression system [Barnhill et al., 2004]. In the present report, we use a novel anti-RGA to isolate physiological complexes between this protein and TRPV2. Our data suggest that the TRPV2/RGA interaction takes place intracellularly, and that RGA does not accompany TRPV2 to the cell surface. The subcellular localization of RGA is unaffected by cAMP, suggesting that this protein does not participate in the final regulated trafficking step that introduces TRPV2 to the plasma membrane. However, we report that RGA overexpression potentiates TRPV2 surface localization. We propose that RGA may regulate the ability of TRP channels to attain the cell surface, and should be considered as a key component of expression systems that seek to elucidate the physiological characteristics of TRPV2.

METHODS

Expression Constructs

Rat TRPV2 cDNA [Caterina et al., 1997, 1999] was sub-cloned into pcDNA4TO (Invitrogen, Carlsbad, CA) with primers that conferred an amino-terminal FLAG epitope tag. The C2.3 (RGA) cDNA [Tagoh et al., 1996] was subcloned into pcDNA5TO (Invitrogen) using primers that conferred a carboxy-terminal V5 epitope tag. All constructs were verified by sequencing.

Antibody Generation

A carboxy-terminal peptide epitope was selected from murine RGA on the basis of predicted antigenicity (MacVector, Accelrys, San Diego, CA), and a high degree of similarity between the murine and rat protein sequences for RGA in this region. The epitope peptide sequence was LGLFCKYPPEQDRKRLLQT. A rabbit polyclonal antibody was generated and affinity purified (Bethyl Laboratories, Montgomery, TX).

Northern Analysis

Multiple cell line Northern blots were produced using 1 μg/lane poly A^+ mRNA isolated from the indicated cell lines via oligo-dT capture. The cDNA probe for TRPV2 was 353 bp,

and was generated by a *Hinc*II/*Not*I digest. Probes were ^{32}P-labeled using random priming. Membranes were hybridized with radiolabeled probe for 2 h/65°C. After two washes in 2× SSC/0.05% SDS/RT for 20 min and two washes in 0.1× SSC/0.1% SDS/50°C for 20 min, membranes were autoradiographed or imaged using a Cyclone Phosphorimager (Perkin Elmer, Madison, WI).

Mammalian Cell Culture and Stable Cell Line Generation

HEK293 cells stably transfected with the pcDNA6TR (Invitrogen) plasmid (encoding the tetracycline-sensitive TRex repressor protein) were maintained in DMEM with 10% fetal bovine serum (inactivated at 55°C for 1 h) supplemented with 2 mM glutamine. Cells were cultured in a humidified 5% CO_2 atmosphere at 37°C. Selection pressure on the TRex 293 cells was maintained using 10 μg/ml Blasticidin (Sigma, St. Louis, MO). For production of Trex HEK293 cells with inducible expression of TRPV2, parental cells were electroporated with each cDNA in pcDNA$_4$TO and clonal cell lines were selected by limiting dilution in the presence of 400 μg/ml Zeocin (Invitrogen) [Barnhill et al., 2004; Stokes et al., 2004]. TRPV channel expression was induced using 1 μg/ml tetracycline for 16 h/37°C. Stable lines were screened for inducible protein expression using Western blot.

Lysis, Immunoprecipitation, and Western Blotting

Cells were pelleted (2,000*g*, 2 min) and washed once in ice-cold PBS. Approximately 10^7 cells were lysed (ice, 30 min) in 350 μl of lysis buffer (50 mM HEPES, pH 7.4, 75 mM NaCl, 20 mM NaF, 10 mM iodoacetamide, 0.5% (w/v) Triton X-100, 1 mM phenylmethylsulfonyl fluoride (PMSF), 500 μg/ml aprotinin, 1.0 mg/ml leupeptin, and 2.0 mg/ml chymostatin). Lysates were clarified (10,000*g*, 5 min). Supernatants were either mixed with 1.4 volumes acetone (−20°C for 1 h to pellet total protein) or tumbled (4°C for 2 h) with the indicated antibody for immunoprecipitation. Acetone precipitates were harvested by centrifugation at 10,000*g* for 5 min. Immunocomplexes were captured using 15 μl protein G-sepharose beads and washed twice in 1 ml lysis buffer. Samples were incubated (95°C for 8 min) in reducing SDS–PAGE buffer. Immunocomplexes were resolved by 10% SDS–PAGE in 25 mM Tris, 192 mM glycine, 0.05% (w/v) SDS, pH 8.8. Resolved proteins were electro-transferred to PVDF. For Western blotting, membranes were blocked using 5% non-fat milk/PBS/1 h/RT. Primary antibodies were dissolved in PBS/0.05% Tween-20/0.05% NaN_3 and incubated with membrane for 16 h at 4°C. Developing antibodies (anti-rabbit or anti-mouse IgGs conjugated to horseradish peroxidase (HRP), Amersham, Piscataway, NJ) were diluted to 0.1 μg/ml in PBS/0.05% Tween-20 and incubated with membranes for 45 min at RT. Standard washes (4 × 5 min in 50 ml PBS/0.1% Tween-20 at RT) occurred between primary and secondary antibodies and following secondary antibody. Signal was visualized using enhanced chemiluminescence (ECL, Amersham). Anti-FLAGM2 and anti-V5 were obtained from Sigma and Invitrogen, respectively. Gel images were scanned and cropped using Adobe Photoshop. Molecular weights standards are provided as guides, actual weights were calculated as R_f values on the basis of the migration and compared to the predicted MW for the protein species.

Cell Surface Biotinylation

Intact cells were incubated (30 min at RT) with 100 μg/ml sulfo-NHS-biotin (Pierce, Rockford, IL) in PBS (pH 8.0) on a rotating mixer. This procedure modifies the NH_2 groups of accessible external lysine residues. Cells were washed four times in 25 mM Tris buffered saline (pH 7.4) (to quench further biotinylation of internal proteins following lysis), transferred to new tubes, and then lysed as above with the addition of 25 mM NH_4Cl to the lysis buffer. Biotinylated proteins were resolved by SDS–PAGE, transferred to PVDF, and visualized using either Streptavidin HRP (1:50,000, Sigma) or anti-biotin HRP at 0.1 μg/ml (Cell Signaling Technologies, Beverley, MA) and ECL (Amersham).

Transient Transfection

Trex HEK293 cells (Invitrogen) were seeded and grown until 50% confluent. All cDNA was purified using a Plasmid Maxi Kit (Qiagen, Valencia, CA). The cDNA quality was measured using a spectrophotometer and used in transfection only if OD 260/280 > 1.7. HEK293 cells were transiently transfected using reagent LT1 (Mirus, Madison, WI). Serum free DMEM (100 μl) and LT1 reagent (10 μl) were added together and vortexed for 30 s. The mixture was

then left at room temperature for 15 min. After 15 min, the cDNA was added to the mixture and mixed gently. After 15 min at RT, the mixture was added to the cells in a drop-wise manner while swirling the plate. The cells were then placed in a humidified 5% CO_2 incubator for 48–72 h. The cells were then harvested and lysed as described above.

Immunofluorescence

Cells were grown on glass coverslips and then fixed (4% paraformaldehyde in PBS, 20 min, RT). Cells were then permeabilized (0.4% Triton X-100 for 4 min at RT). After blocking (0.7% fish skin gelatin in PBS, 20 min, RT), coverslips were incubated with primary and secondary antibodies (30 min each, RT) and Hoechst 33342 1 μg/ml for 2 min at RT (Molecular Probes, Eugene, OR). Where indicated, cell bodies were delineated using 1 μM Cell Tracker green (Molecular Probes). Coverslips were washed four times in PBS between each stage of antibody exposure. After mounting (CrystalMount, Biomeda, Foster City, CA) imaging was per-

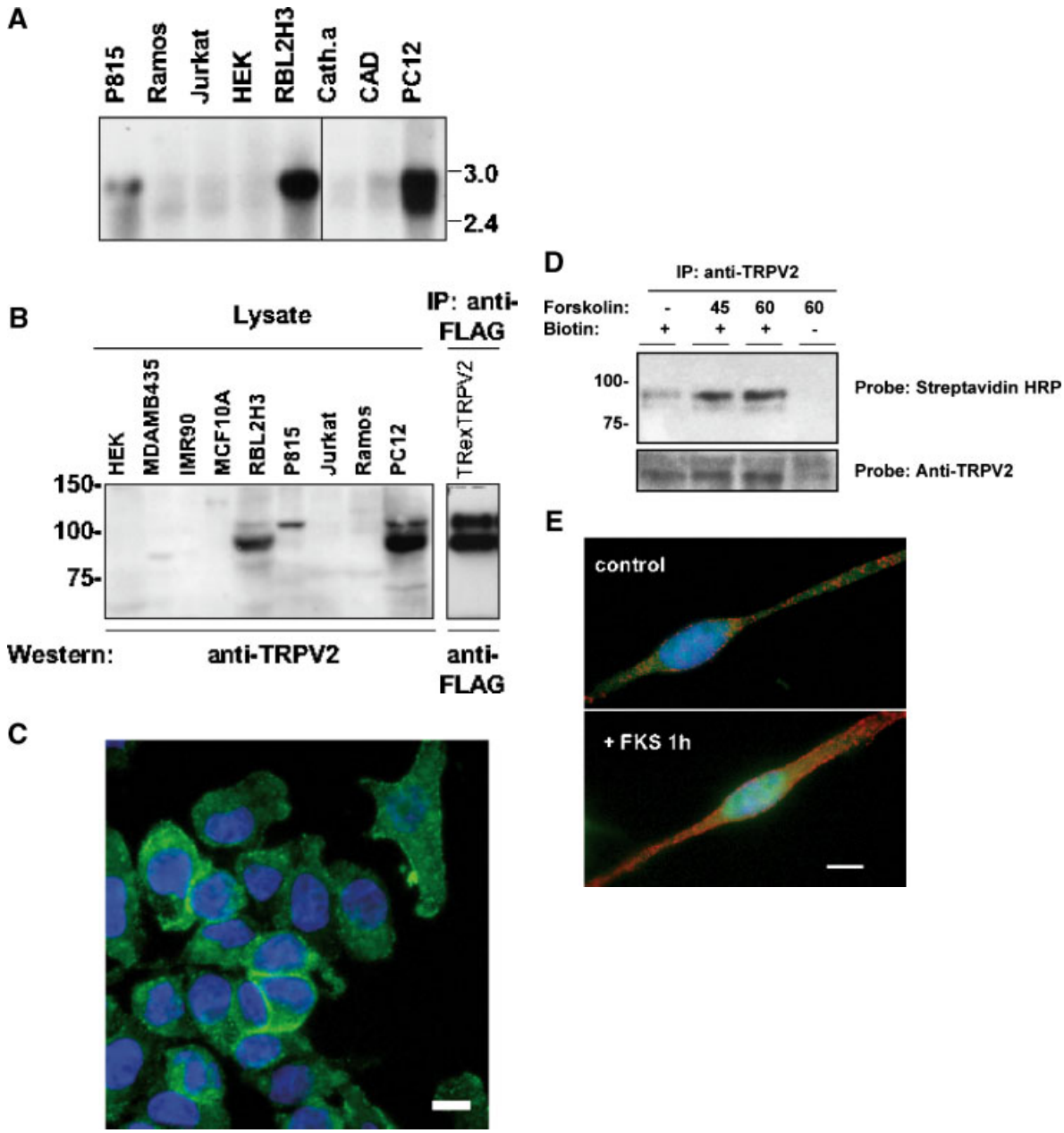

Fig. 1.

formed with an Olympus IX70 fluorescence inverted microscope with quadruple dichroic filter block and excitation filters (filter set 88000, Chroma, Rockingham, VT). F-view monochrome CCD camera, framegrabber, and camera control software (Microsuite) were from Soft Imaging Systems (Melville, NY).

RESULTS

cAMP-Regulated Trafficking Step Brings TRPV2 to the Cell Surface

Mast cells are native expression contexts for the TRPV2 cation channel. This property is shared by the transformed mast cell lines RBL2H3 and P815, which express abundant transcripts for TRPV2 (Fig. 1A). Moreover, the Western analysis in Figure 1B shows that both RBL2H3 and P815, mast cell lines express a protein doublet that migrates similarly to heterologously-expressed TRPV2, and which is recognized by an anti-TRPV2 antibody [Barnhill et al., 2004; Stokes et al., 2004]. We have focused upon RBL2H3 as a model cellular system in which to explore the biology of TRPV2.

TRPV2 is believed to function as a cation channel that conducts current across the plasma membrane. However, TRPV2 may not reside at the plasma membrane of resting cells. Several groups have reported that the murine TRPV2 homolog, GRC, can be recruited to the surface of myocytes (in response to stretch), insulinoma cells (following exposure to growth factors), and neuroendocrine cells (in response to a specific neuropeptide) [Kanzaki et al., 1999; Boels et al., 2001; Iwata et al., 2003]. We therefore asked if a similar mechanism promoted surface localization of rat TRPV2 in RBL2H3 mast cells. Initially, we examined the subcellular localization of TRPV2 in resting RBL2H3 mast cells using immunocytochemistry. We noted that coronal staining for TRPV2, an indicator of surface expression, was only present, weakly, in a sub-population of resting RBL2H3 cells (Fig. 1C). These data suggest that a specific activation event may be necessary in mast cells to complete the trafficking of TRPV2 and insert the channel into the plasma membrane.

We established a surface biotinylation protocol in order to accurately assess the amount of TRPV2 in the plasma membrane of RBL2H3. This technique relies on the biotinylation of exposed lysine residues in the extracellular domains of TRPV2. Topological predictions for

Fig. 1. **A**: Northern analysis of transient receptor potential, sub-family Vanilloid (TRPV2) transcripts in cell lines. Multiple cell line Northern blots were produced using 1 μg poly A^+ mRNA per lane. These blots were probed with a ^{32}P-labeled cDNA fragment corresponding to a 353 bp fragment (*Hin*cII/*Not*I) derived from rat TRPV2. Strong hybridization of a single band of approximately 2.8 kb was visible after 16 h exposure to storage phosphor screens. RNA was derived from the following cell lines: p815, murine mastocyoma; Ramos, human B lymphoma; Jurkat, human T leukemia; HEK, human embryonic kidney fibroblast; RBL2H3, rat basophilic leukemia; Cath/CAD, murine catecholaminergic neuron; PC12, rat pheochromocytoma. **B**: Western analysis of TRPV2 protein in cell lines. **Left panel**: Lysates were prepared from 1×10^6 of the indicated cell lines and total protein was prepared via acetone precipitation. Protein samples were normalized using a Bradford assay and resolved under reducing conditions on 10% SDS–PAGE. After electrotransfer, TRPV2 bands were visualized by Western blot with 0.1 μg/ml anti-TRPV2 (Oncogene, San Diego, CA). Predicted MW of unmodified TRPV2 is 97 kDa. IMR90, human lung fibroblast; MDA/MCF, human breast epithelial fibroblast. **Right panel**: TRexTRPV2 cells, with FLAG-TRPV2 expression under the control of a tetracycline-sensitive transcriptional repressor, were constructed. TRexTRPV2 were exposed to vehicle or 1 μg/ml tetracycline for 16 h at 37°C, to induce expression of FLAG-TRPV2. Triton X-100 lysates from 1×10^7 TRexTRPV2 cells were immunoprecipitated with 2 μg anti-FLAG. Immunocomplexes were resolved by 10% SDS–PAGE and electrotransferred. FLAG-TRPV2 was visualized by Western blotting in 0.6 μg/ml anti-FLAG antibody. **C**: Anti-TRPV2 immunofluorescence in resting RBL2H3 cells. Anti-TRPV2 immunofluorescence in resting RBL2H3 was evaluated. Efficacy of the anti-TRPV2 in this application was verified by dual staining of TRExTRPV2 cells with anti-FLAG and anti-TRPV2 (data not shown). Anti-TRPV2 was used at 0.1 μg/ml, and visualized using an Alexa-488 conjugated anti-rabbit secondary antibody (green fluorescence). Nuclei were counter-stained with Hoechst 33342 (1 μg/ml) (blue fluorescence). Scale bar indicates 10 μm. **D**: Surface biotinylation of TRPV2 in resting and FKS-treated RBL2H3 cells. RBL2H3 were treated with 25 μM Forskolin for the indicated times (in min) at 37°C. Intact RBL2H3 (5×10^7 cells) were surface biotinylated. Biotinylation reactions were quenched with 25 mM NH_4Cl. Lysates were immunoprecipitated with 10 μg anti-TRPV2, and immunocomplexes were resolved by 10% SDS–PAGE. After electrotransfer, biotinylated proteins were visualized using streptavidin–horseradish peroxidase (HRP) conjugate (**upper panel**), while immunoprecipitated TRPV2 was visualized using an anti-TRPV Western blot (**lower panel**). **E**: Subcellular localization of TRPV2 immunofluorescence in resting and FKS-treated cells. RBL2H3 were treated with vehicle or 25 μM Forskolin for 60 min at 37°C. Anti-TRPV2 immunofluorescence was evaluated. Efficacy of the anti-TRPV2 in this application was verified by dual staining of TRExTRPV2 cells with anti-FLAG and anti-TRPV2 (data not shown). Anti-TRPV2 was used at 0.1 μg/ml, and visualized using an Alexa-568 conjugated anti-rabbit secondary antibody. Cell bodies were delineated using 1 μM Cell Tracker green. Nuclei were counter-stained with Hoechst 33342 (1 μg/ml). Scale bar indicates 10 μm. [Color figure can be viewed in the online issue, which is available at www.interscience.wiley.com.]

rat TRPV2 suggest two candidate lysines (K426, K566) for this modification [Caterina et al., 1999], both contained within the predicted extracellular loops that separate transmembrane domains. We were able to surface biotinylate a small population of TRPV2 in resting RBL2H3 cells (Fig. 1D). We screened various stimuli for the potential to increase plasma membrane levels of TRPV2 in this cell system, including IGF-1 [Kanzaki et al., 1999], EGF, ligation of the FcεRI immunoreceptor [Turner and Kinet, 1999], phorbol esters and ionomycin. We did not observe a detectable increase in surface levels of TRPV2 in response to any of these agents (data not shown). However, treatment with the cAMP mobilizing agent, Forskolin, caused a dramatic increase in the apparent surface levels of TRPV2 (Fig. 1D), over a 40–60 min time course. We noted that both slower and faster migrating forms of TRPV2 attain the cell surface. Treatment with Forskolin induced a measurable increase in cAMP levels (data not shown), which averaged 5.5 pmoles (±1.3 pmoles) cAMP, above baseline levels, per 10,000 cells at 60 min exposure ($n = 3$). Relocalization of TRPV2 in response to Forskolin was notable in immunofluorescence staining of a subset of cells, exemplified in Figure 1E. These data suggest that access of TRPV2 to the cell surface is indeed controlled in mast cells, and that the physiological stimulus that drives TRPV2 surface localization may be mimicked by elevations in intracellular cAMP.

Polyclonal Antibody That Specifically Detects RGA

We have previously shown that the RGA protein interacts with TRPV2 [Barnhill et al., 2004]. We hypothesized that this interaction occurs intracellularly, and that RGA is involved in TRPV2 biogenesis and/or trafficking. In our previous publication, we showed that heterologously-expressed, epitope tagged, RGA was present in immunocomplexes that were isolated from RBL2H3 using anti-TRPV2. In order to demonstrate that RGA and TRPV2 associate in native immunocomplexes, we sought to develop and validate an antibody to the RGA protein.

A carboxyl-terminal peptide epitope was identified in the murine RGA sequence, and used to immunize rabbits. The resulting antiserum was affinity purified and evaluated as shown in Figure 2. TRex (Invitrogen) HEK293 cells were stably transfected with the RGA cDNA under the control of a tetracycline-sensitive transcriptional repressor. The RGA cDNA was modified by the addition of an amino-terminal V5 epitope tag. Figure 2A shows that tetracycline addition to the TRexRGA cells induces the expression of a 23 kDa protein that may be immunoprecipitated, and visualized, via the V5 epitope tag. This V5-RGA protein can be Western blotted using the novel RGA antibody described above. These data suggest that the novel anti-RGA is effective in recognizing immunoprecipitated RGA protein. We asked if anti-RGA could detect RGA in lysates containing total protein derived from either human tissues or cultured cells. Figure 2B shows that anti-RGA detects a 23 kDa protein in brain, small intestine, skeletal muscle, and pancreatic tissue samples. We also probed lysates derived from immortalized cell lines for expression of RGA. Figure 2C shows that the mast cell lines RBL2H3 (rat) and P815 (mouse), express significant amounts of endogenous RGA protein.

RGA and TRPV2 Associate in a Native Complex

Few protein–protein interactions have been characterized for TRPV cation channels. We have previously documented an interaction between TRPV2 and RGA. Initially, this interaction was suggested by a yeast two-hybrid screen. We subsequently showed that, in a transfection system, over-expressed TRPV2 and RGA do interact at the protein level. Figure 3A demonstrates this interaction. Here, TRex HEK cells that stably express FLAG-TRPV2 were re-transfected with a construct containing V5-RGA. Anti-V5 immunoprecipitates contain a FLAG-reactive protein that apparently corresponds to the faster migrating form of TRPV2. Figure 3B shows that treatment of lysates with peptide *N*-glycosidase F (PNGase F, cleaves innermost sugar linkage between oligosaccharides and N-linked glycoproteins) causes loss of the slower migrating (higher molecular weight) form of TRPV2, suggesting that this is a glycoform [Kedei et al., 2001; Jahnel et al., 2003; Barnhill et al., 2004].

We used the novel anti-RGA to ascertain whether TRPV2 and RGA can be co-immunoprecipitated from a native expression context, the RBL2H3. Figure 3C shows that anti-TRPV2 immunoprecipitates, prepared from RBL2H3, contain both TRPV2 and a small amount of RGA

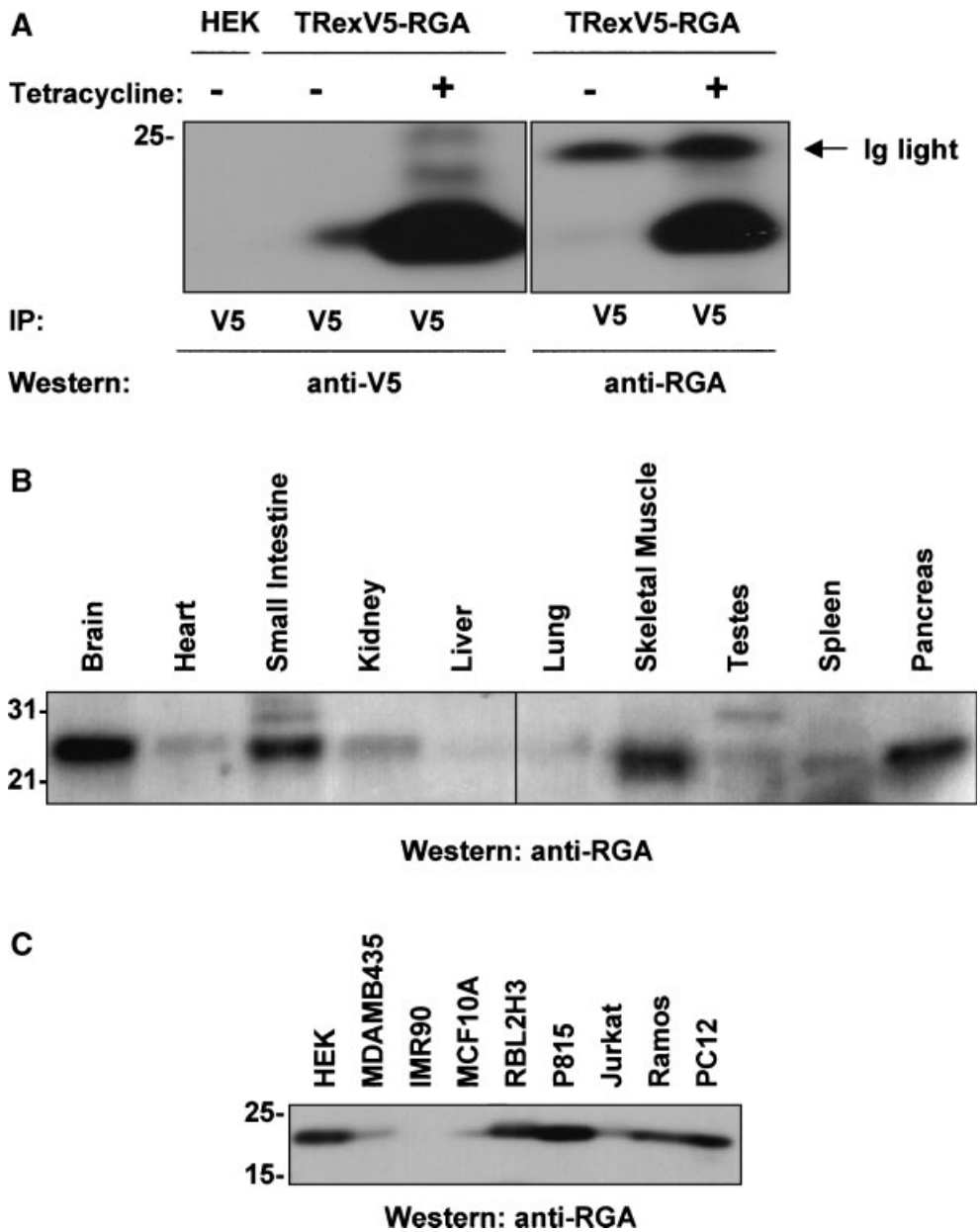

Fig. 2. **A**: Novel anti-recombinase gene activator (RGA) antibody recognizes RGA protein in an over-expression system. TRexRGA cells, with V5-RGA expression under the control of a tetracycline-sensitive transcriptional repressor, were constructed. TRexRGA were exposed to vehicle or 1 μg/ml tetracycline for 16 h at 37°C, to induce expression of V5-RGA. Triton X-100 lysates from 1×10^7 TRexRGA cells were immunoprecipitated with 2 μg anti-V5. Immunocomplexes were resolved by 10% SDS–PAGE and electrotransferred. V5-RGA was visualized by Western blotting in 0.5 μg/ml anti-V5 antibody (**left panel**) or 1 μg/ml anti-RGA (**right panel**). **Second lane** of left-hand panel displays some signal carry-over. **B**: Novel anti-RGA antibody recognizes a 24 kDa protein in various human tissues. A multiple tissue Western blot (Calbiochem, San Diego, CA) was probed using 1 μg/ml anti-RGA. Antibody binding was visualized using an HRP-conjugated anti-rabbit secondary antibody followed by enhanced chemiluminescence (ECL). Predicted molecular weight of unmodified RGA is 24 kDa. **C**: Novel anti-RGA antibody recognizes a 24 kDa protein in various immortalized cell lines. Lysates were prepared from 1×10^6 of the indicated cell lines and total protein was prepared via acetone precipitation. Protein samples were normalized using a Bradford assay and resolved under reducing conditions on 10% SDS–PAGE. After electrotransfer, RGA bands were visualized by Western blot with 1 μg/ml anti-RGA. Predicted molecular weight of unmodified RGA is 24 kDa.

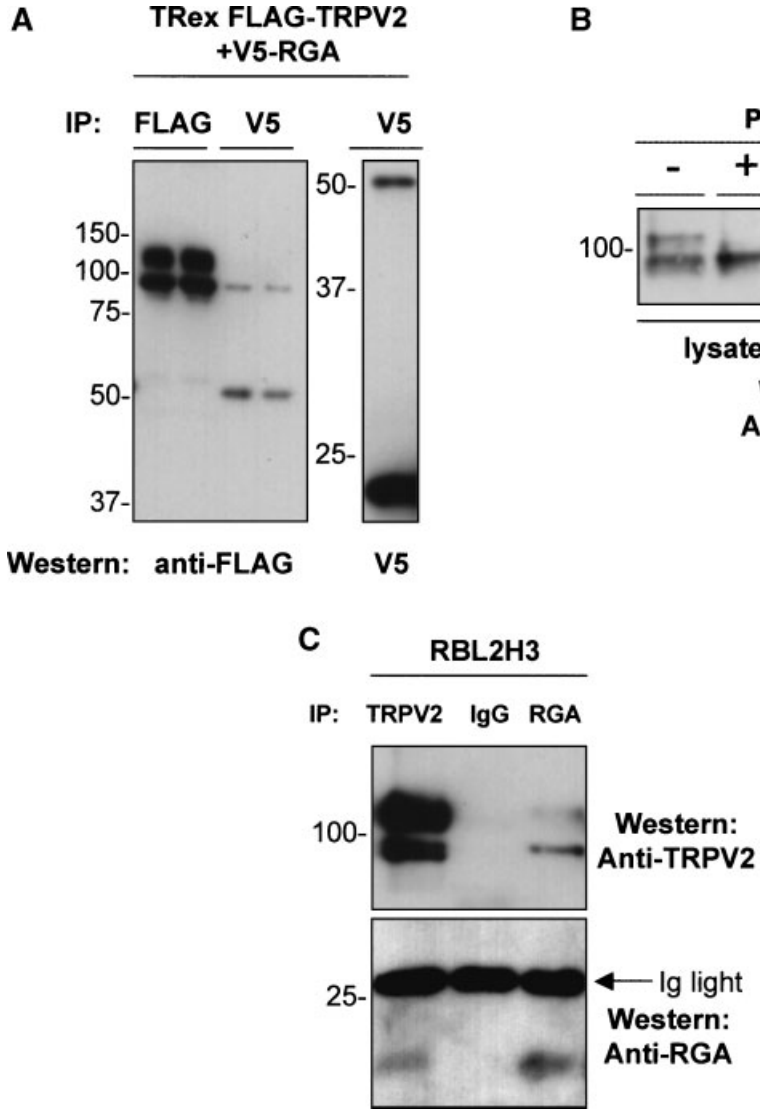

Fig. 3. **A**: Co-immunoprecipitation of over-expressed TRPV2 and RGA proteins. TRexFLAG-TRPV2 cells were transiently re-transfected with the V5-RGA construct. Cells were exposed to vehicle or 1 μg/ml tetracycline for 16 h at 37°C, to induce expression of FLAG-TRPV2. Triton X-100 lysates from 1×10^7 cells were immunoprecipitated with either 0.5 μg anti-FLAG or 2 μg anti-V5. Immunocomplexes were resolved by 10% SDS–PAGE and electrotransferred. FLAG-TRPV2 was visualized by Western blotting in 0.1 μg/ml anti-FLAG antibody (**left panel**), while degree of expression of transfected V5-RGA was assessed by anti-V5 Western blot on a duplicate gel (0.5 μg/ml) (**right panel**). **B**: Deglycosylation results in loss of the faster migrating TRPV2 band from protein samples. RBL2H3 cells were lysed in buffer supplemented with 500 μg/ml aprotinin, 1.0 mg/ml leupeptin, and 2.0 mg/ml chymostatin. Lysates were incubated in the absence or presence of 10 mU peptide *N*-glycosidase F (PNGase F) per 400 μl lysis buffer for 4 h at 35°C. Total protein was harvested by acetone precipitation (**left panel**) or anti-TRPV2 immunocomplexes were prepared using 4 μg per sample anti-TRPV2 (**right panel**). Samples were resolved by 10% SDS–PAGE and Western blotted using anti-TRPV2 (0.1 μg/ml). **C**: Co-immunoprecipitation of TRPV2 and RGA from RBL2H3 cells. Lysates from 2×10^7 RBL2H3 cells were used to prepare the immunocomplexes shown. Immunoprecipitation was performed with either 4 μg anti-TRPV2 or 6 μg anti-RGA. As a control a mock precipitation was performed with 10 μg rabbit immunoglobulins. Immunocomplexes were captured with Protein A-agarose and resolved by 10% SDS–PAGE. After electrotransfer, the membrane was divided at the 50 kDa marker and probed with either 0.1 μg/ml anti-TRPV2 (**upper panel**) or 1 μg/ml anti-RGA (**lower panel**).

protein. Moreover, anti-RGA immunoprecipitates contain both RGA and both species of the TRPV2 protein doublet. Within this doublet, the higher mobility form of TRPV2 predominates, but there is less of a bias toward the faster migrating form of TRPV2 that we observe in our over-expression system. Taken together, these data suggest that RGA and TRPV2 form a physiological complex in RBL2H3 mast cells.

RGA Does not Attain the Cell Surface in RBL2H3 Mast Cells

The data presented above suggest that RGA preferentially associates with an unglycosylated form of TRPV2. We have previously proposed that the V5-RGA protein associates with TRPV2 intracellularly, during TRPV2 biosynthesis and trafficking, since V5-RGA presents an immunocytochemical staining pattern that is consistent with localization to the ER/Golgi apparatus [Barnhill et al., 2004]. In the current report, we asked whether endogenous RGA attains the cell surface.

RGA contains several lysine residues in both of the proposed extracellular loops that separate its transmembrane helices. Both rat and mouse RGA sequences share K94, K150, and K155 in the putative extracellular regions. The presence of these lysine residues suggests that RGA would be amenable to surface biotinylation if it attains the cell surface and these loops are exposed. Figure 4A shows that, as described above for native TRPV2 in RBL2H3, FLAG-TRPV2 may be readily surface biotinylated in TRexTRPV2 cells. Re-transfection of these cells with the V5-RGA construct results in the appearance of a prominent 23 kDa protein (Fig. 4B). However, this V5-RGA does not react with an anti-biotin antibody (Fig. 4B), even when prepared from surface biotinylated cells. In contrast, RGA is readily biotinylated in cell lysates [Barnhill et al., 2004] (and data not shown). We also used a streptavidin–agarose matrix to affinity purify proteins from surface biotinylated RBL2H3 mast cells. Probing of these precipitates with the anti-RGA antibody did not reveal any detectable native RGA protein (data not shown). Taken together, these data suggest that V5-RGA does not attain the cell surface to a significant degree and support the hypothesis that the TRPV2/RGA interaction is intracellular.

We assayed the subcellular localization of endogenous RGA protein in RBL2H3 mast cells, in order to ascertain whether RGA is likely to localize to the plasma membrane in a native expression system. Figure 4C shows that anti-RGA immunofluorescence in RBL2H3 is predominantly localized in a perinuclear structure. This structure is stained by both anti-RGA and anti-V5 in V5-RGA transfected cells (data not shown). The observed staining pattern for RGA is not consistent with localization of this protein to the cell surface, but rather suggests that RGA is present in the perinuclear Golgi apparatus and endoplasmic reticulum.

The data presented in Figure 1D,E show that cAMP elevations, achieved via application of Forskolin, cause surface accumulation of TRPV2 protein. Since we propose that RGA is a component of the TRPV2 trafficking pathway, we asked whether RGA also exhibits a cAMP-sensitive subcellular localization. We evaluated the localization pattern for RGA in the absence and presence of the cAMP-mobilizing agent, Forskolin. Figure 4D shows that the subcellular localization of RGA protein is not altered when RBL2H3 are exposed to Forskolin, despite the marked effect that this reagent has upon TRPV2 localization. Taken together, these data support the idea that RGA does not accompany TRPV2 to the cell surface or participate in the late, cAMP regulated, trafficking step that places TRPV2 in the plasma membrane.

RGA Expression Potentiates Surface Localization of TRPV2

RGA and TRPV2 form a complex that can be immunoprecipitated from RBL2H3 mast cells. The purpose of the interaction between these two proteins remains unclear. No similar interaction partners have been documented for TRP channels, and while regulated access to the cell surface is postulated for several family members, intracellular proteins that participate in the controlled trafficking of TRPs have not been identified. Two types of accessory protein interaction have been described for channels outside the TRP family, including interactions that potentiate cell surface access, and those which tend to retain the channel in the ER/Golgi apparatus. We hypothesized that interaction with RGA may perform one of these functions within the TRPV2 trafficking pathway.

We asked if the presence of RGA protein caused a change in the amount of TRPV2 that attained the cell surface in TRexTRPV2 cells. These cells were transiently re-transfected with either empty plasmid or with the V5-RGA construct. Intact cells were surface-labeled with biotin and TRPV2 was immunoprecipitated via the FLAG tag. The upper panel of Figure 5A shows that tetracycline addition to TRexTRPV2 cells induces the enhanced expression of the FLAG-tagged TRPV2 protein doublet. Surface expression of TRPV2 is detectable in both uninduced and tetracycline-treated TRexTRPV2

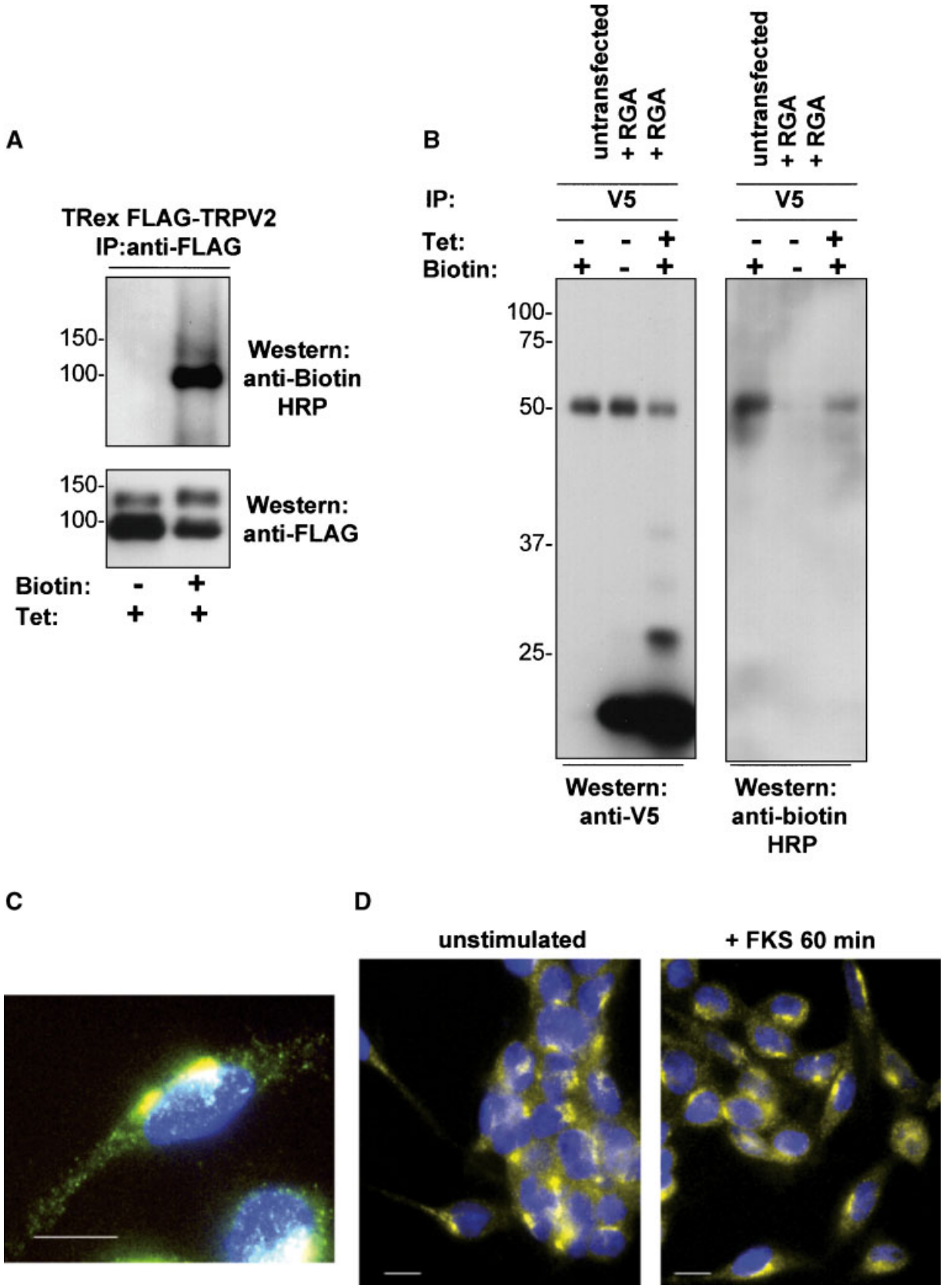
A
TRex FLAG-TRPV2
IP:anti-FLAG
150-
100-
Western:
anti-Biotin
HRP
150-
100-
Western:
anti-FLAG
Biotin: - +
Tet: + +
B
untransfected
+ RGA
+ RGA
untransfected
+ RGA
+ RGA
IP:
V5
V5
Tet: - - + - - +
Biotin: + - + + - +
100-
75-
50-
37-
25-
Western:
anti-V5
Western:
anti-biotin
HRP
C
D
unstimulated
+ FKS 60 min

Fig. 4.

cells. Interestingly, we observe a marked increase in the levels of biotinylated TRPV2 in cells that over-express V5-RGA (Fig. 5A, lower panel, and Fig. 5B).

We asked whether an increase in cellular levels of RGA affected the amount of endogenous TRPV2 at the surface of RBL2H3. Figure 5C shows that RBL2H3 contain a significant amount of surface biotinylated TRPV2, purified using an anti-TRPV2 immunoprecipitation. When transfected with V5-RGA, these cells display a marked increase in surface TRPV2 levels (upper panel), without a concomitant increase in total TRPV2 (lower panel). Figure 5D confirms the levels of V5-RGA that were present in untransfected and transfected cells, respectively. Taken together, these data suggest that RGA over-expression positively correlates with surface levels of TRPV2 in mast cells.

DISCUSSION

Regulated trafficking to the plasma membrane has been proposed as a component of the activation pathway for the murine TRPV2 homolog, GRC. This potential level of regulation has been described in non-sensory cells [Kanzaki et al., 1999; Boels et al., 2001; Muraki et al., 2003]. TRPV2 is also expressed in multiple immune system tissues, including mast cells. In the present report we show that an elevation in cytosolic cAMP levels, provided over a 40–60 min time course, causes TRPV2 to accumulate in the plasma membrane of a rat mast cell line. These data suggest that a regulated trafficking step operates for rat TRPV2 and is a component of the activation process for TRPV2 in mast cells. Mobilization of cAMP is not known to be an acute outcome of either IGF-1 or neuropeptide HA stimulation, both of which stimulate GRC translocation in certain cells [Kanzaki et al., 1999; Boels et al., 2001]. A common link between the stimuli that have been documented to induce TRPV2 translocation therefore remains to be elucidated. Interestingly, the regulated translocation step does not appear to be required for TRPV2 function in sensory neurons or in over-expression systems. Here, acute heat stimulation appears to activate channels within seconds of application, suggesting that there is a basal plasma membrane population of TRPV2 in these cells [Caterina et al., 1999; Jordt and Julius, 2002; Jahnel et al., 2003]. It is possible that the basal levels of TRPV2 in the membranes of neuronal cells are established by a cAMP-dependent trafficking mechanism that operates at a distinct point in the proliferation or differentiation process, prior to the receipt of an acute stimulus. We consistently note a small basal population of TRPV2 in the mast cell plasma membrane, which may be established via a similar mechanism, and which we have shown does confer a heat-activated calcium signal upon these cells [Stokes et al., 2004]. Thus in these, and potentially other peripheral cells, plasma membrane TRPV2 is activatable via elevated temperature. However, it seems likely that an alternate activation pathway is the physiological stimulus for TRPV2 in non-sensory cells.

Description of the protein–protein interactions made by ion channels may provide insight into their potential regulatory mechanisms and physiological roles. In the present report, we examined the interaction between TRPV2 and RGA [Tagoh et al., 1996], an intracellular protein with four-transmembrane domains.

Fig. 4. **A**: Surface biotinylation of FLAG-TRPV2. TRexFLAG-TRPV2 cells were treated with tetracycline for 16 h to induce expression of FLAG-TRPV2. Intact cells were surface biotinylated. Immunocomplexes were isolated using 2 μg anti-FLAG and resolved by 10% SDS–PAGE on duplicate gels. After electrotransfer, the duplicate membranes were probed with either anti-biotin HRP (0.5 μg/ml, **upper panel**) or anti-FLAG (**lower panel**). **B**: V5-RGA protein is not surface biotinylated. TRexFLAG-TRPV2 cells were transiently transfected with V5-RGA or left untransfected. Tetracycline treatment was performed as indicated, to induce expression of FLAG-TRPV2. Intact cells were then surface biotinylated as described above. Immunocomplexes were isolated using 2 μg anti-V5 and resolved by 10% SDS–PAGE on duplicate gels. After electrotransfer, the duplicate membranes were probed with either anti-V5 (**left panel**) or anti-biotin HRP (**right panel**). **C**: Anti-RGA immunofluorescence in resting RBL2H3 cells. Anti-RGA immunofluorescence in resting RBL2H3 was evaluated. Efficacy of the anti-RGA in this application was verified by dual staining of V5-RGA transfected cells with anti-V5 and anti-RGA (data not shown). Anti-RGA was used at 0.1 μg/ml, and visualized using an Alexa-488 conjugated anti-rabbit secondary antibody (green fluorescence). Nuclei were counter-stained with Hoechst 33342 (blue fluorescence) (1 μg/ml). Scale bar indicates 10 μm. **D**: Anti-RGA immunofluorescence in resting and FKS-treated RBL2H3 cells. RBL2H3 were treated with vehicle (**left panel**) or 25 μM forskolin (**right panel**) for 60 min at 37°C. Anti-RGA immunofluorescence in resting RBL2H3 was evaluated. Efficacy of the anti-RGA in this application was verified by dual staining of V5-RGA transfected cells with anti-V5 and anti-RGA (data not shown). Anti-RGA was used at 0.1 μg/ml, and visualized using an Alexa-488 conjugated anti-rabbit secondary antibody. Nuclei were counter-stained with Hoechst 33342 (1 μg/ml). [Color figure can be viewed in the online issue, which is available at www.interscience.wiley.com.]

In a previous report, we documented the results of a yeast two hybrid screen that suggested an interaction between the amino-terminal cytoplasmic tail of TRPV2 and RGA [Barnhill et al., 2004]. Here, we extend these data through the use of a novel antibody to the RGA protein. We use a native expression system for both TRPV2 and RGA to show that these proteins form a physiological complex in mast cells. It remains to be established whether this is a direct, or indirect, protein–protein interaction. Moreover, we confirm that RGA does not attain the

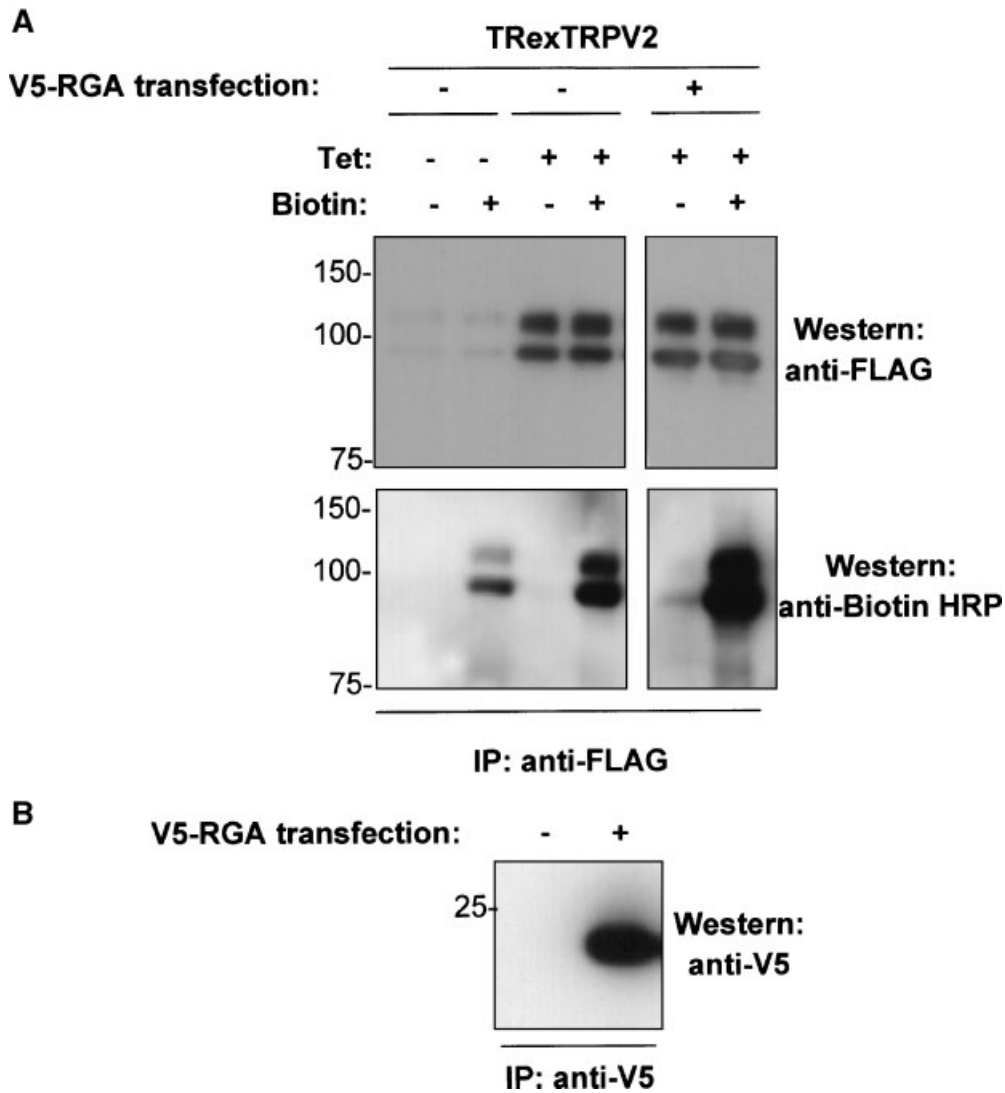

Fig. 5. **A**: RGA expression potentiates the surface localization of FLAG-TRPV2. TRexFLAG-TRPV2 cells were transiently transfected with V5-RGA or left untransfected. Tetracycline treatment was performed as indicated, to induce expression of FLAG-TRPV2. Intact cells were then surface biotinylated as described above. Immunocomplexes were isolated using 2 μg anti-FLAG and resolved by 10% SDS–PAGE on duplicate gels. After electrotransfer, the duplicate membranes were probed with either anti-FLAG (**upper panel**) or anti-biotin HRP (**lower panel**). **B**: Transfection of V5-RGA results in V5-RGA over-expression. This gel confirms expression of V5-RGA in the biotinylation experiment presented as Figure 5A. TRexFLAG-TRPV2 cells were transiently transfected with V5-RGA or left untransfected. Immunocomplexes were isolated using 2 μg anti-V5 and resolved by 10% SDS–PAGE. After electrotransfer, the membrane was probed with anti-V5. **C**: RGA expression potentiates the surface localization of endogenous TRPV2. RBL2H3 were transiently transfected with V5-RGA or left untransfected. Intact cells were then surface biotinylated as described above. Immunocomplexes were isolated using 4 μg anti-TRPV2 and resolved by 10% SDS–PAGE on duplicate gels. After electrotransfer, the duplicate membranes were probed with either anti-biotin HRP (**upper panel**) or anti-TRPV2 (**lower panel**). **D**: Transfection of V5-RGA results in V5-RGA over-expression. This gel confirms expression of V5-RGA in the biotinylation experiment presented as Figure 5C. RBL2H3 were transiently transfected with V5-RGA or left untransfected. Immunocomplexes were isolated using 2 μg anti-V5 and resolved by 10% SDS–PAGE. After electrotransfer, the membrane was probed with anti-V5.

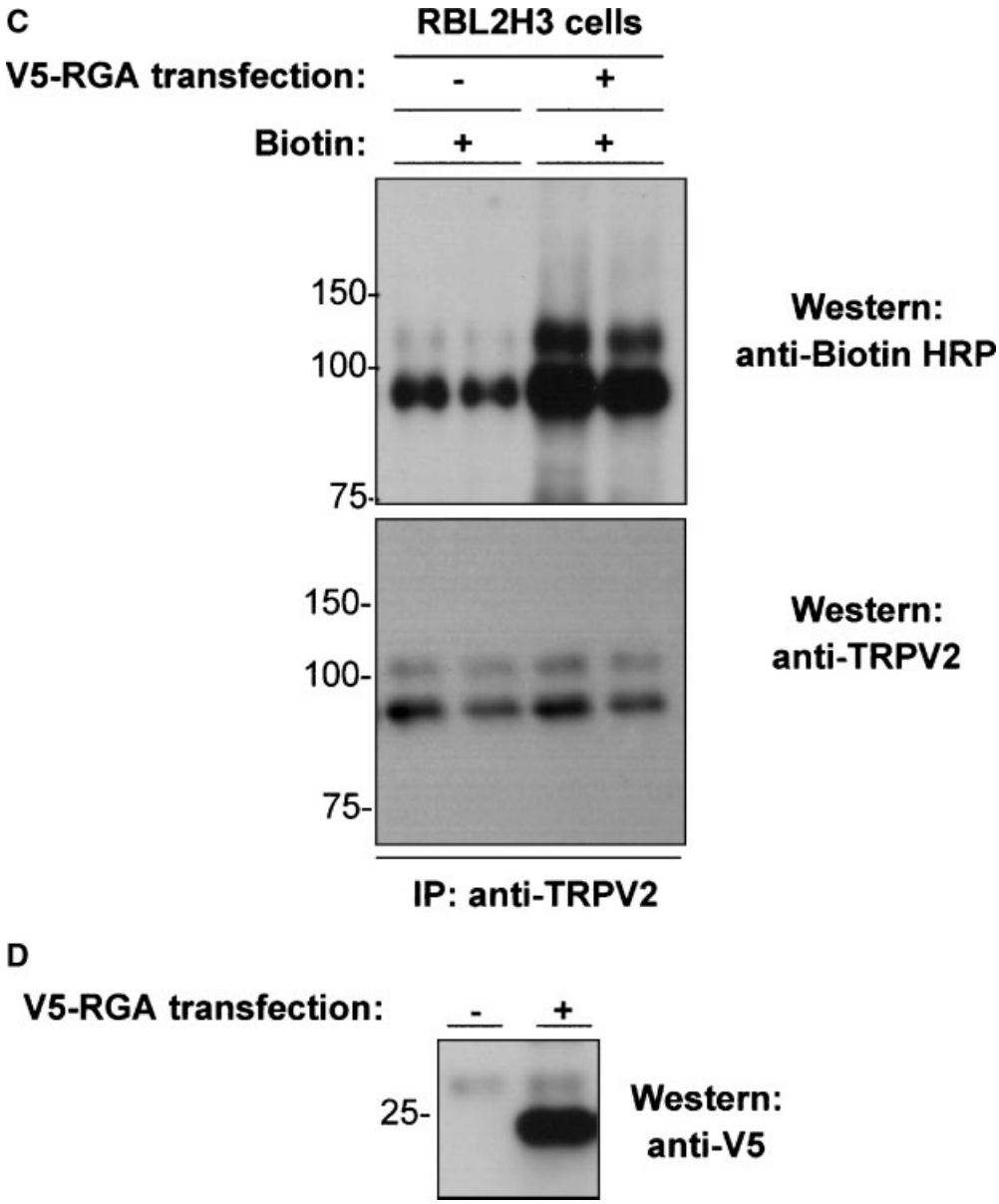

Fig. 5. (*Continued*)

cell surface. Interestingly, over-expression of RGA protein is accompanied by a marked increase in the basal levels of TRPV2 in the plasma membrane. These data suggest that RGA participates in the TRPV2 trafficking pathway, and we propose that RGA itself may be a target for signals that determine surface levels of TRPV2 during development, proliferation, or differentiation.

Tagoh et al. [1996] isolated the RGA cDNA from a B cell library during a screen for cDNAs whose products could induce expression of recombinase activating genes (*RAG*) in a murine B lymphocyte system. RGA is distantly related to the *Drosophila* protein slv [Artero et al., 1998], and the *Medicago truncatula* protein mtn3 [Gamas et al., 1996], neither of which have assigned molecular roles. In mammalian systems, RGA bears topological similarity, and loose sequence homology, to the extensive MS4 family of four-transmembrane domain proteins [Liang et al., 2001; Liang and Tedder, 2001; Barnhill et al., 2004]. Few MS4 proteins have assigned functions, and any interaction with ion channel species has not been demonstrated. Future work will address the questions of whether RGA interacts with channel species other than TRPV2, and

whether its role in trafficking is indicative of a general function for proteins related to RGA.

Taken together, our data suggest that regulated trafficking may be an important aspect of TRPV2 physiology. Trafficking and activation pathways may intersect for other TRP channel species, for example, TRPC4 [Mery et al., 2002]. Interaction with the RGA protein can regulate the levels of TRPV2 that attain the cell surface in resting cells, and these levels can be further enhanced by a cAMP-mobilizing stimulus. The study of TRPV2 may be facilitated by our present findings, since electro-physiological experiments that aim to identify factors that regulate TRPV2 may be redundant if the channel has not previously been induced to enter the plasma membrane.

ACKNOWLEDGMENTS

Linden T. Doescher provided excellent technical assistance with the experiments in this paper. Dr. David Julius (UCSF) generously provided and TRPV2 cDNAs, and Dr. Atsushi Muraguchi (Toyama Medical and Pharmaceutical University) kindly provided the RGA cDNA clone C2.3.

REFERENCES

Artero RD, Terol-Alcayde J, Paricio N, Ring J, Bargues M, Torres A, Perez-Alonso M. 1998. *Saliva*, a new *Drosophila* gene expressed in the embryonic salivary glands with homologues in plants and vertebrates. Mech Dev 75:159–162.

Barnhill JC, Stokes AJ, Koblan-Huberson M, Shimoda LM, Muraguchi A, Adra CN, Turner H. 2004. RGA protein associates with a TRPV ion channel during biosynthesis and trafficking. J Cell Biochem 91:808–820.

Benham CD, Gunthorpe MJ, Davis JB. 2003. TRPV channels as temperature sensors. Cell Calcium 33:479–487.

Boels K, Glassmeier G, Herrmann D, Riedel IB, Hampe W, Kojima I, Schwarz JR, Schaller HC. 2001. The neuropeptide head activator induces activation and translocation of the growth-factor-regulated $Ca^{(2+)}$-permeable channel GRC. J Cell Sci 114:3599–3606.

Bradding P, Conley EC. 2002. Human mast cell ion channels. Clin Exp Allergy 32:979–983.

Caterina MJ, Julius D. 2001. The vanilloid receptor: A molecular gateway to the pain pathway. Annu Rev Neurosci 24:487–517.

Caterina MJ, Schumacher MA, Tominaga M, Rosen TA, Levine JD, Julius D. 1997. The capsaicin receptor: A heat-activated ion channel in the pain pathway. Nature 389:816–824.

Caterina MJ, Rosen TA, Tominaga M, Brake AJ, Julius D. 1999. A capsaicin-receptor homologue with a high threshold for noxious heat. Nature 398:436–441.

Chang W, Gelman MS, Prives JM. 1997. Calnexin-dependent enhancement of nicotinic acetylcholine receptor assembly and surface expression. J Biol Chem 272: 28925–28932.

Clapham DE. 2002. Signal transduction. Hot and cold TRP ion channels. Science 295:2228–2229.

Deutsch C. 2002. Potassium channel ontogeny. Annu Rev Physiol 64:19–46.

Gamas P, Niebel Fde C, Lescure N, Cullimore J. 1996. Use of a subtractive hybridization approach to identify new *Medicago truncatula* genes induced during root nodule development. Mol Plant Microbe Interact 9:233–422.

Gothel SF, Marahiel MA. 1999. Peptidyl-prolyl *cis–trans* isomerases, a superfamily of ubiquitous folding catalysts. Cell Mol Life Sci 55:423–436.

Green WN, Millar NS. 1995. Ion-channel assembly. Trends Neurosci 18:280–287.

Heiner I, Eisfeld J, Halaszovich CR, Wehage E, Jungling E, Zitt C, Luckhoff A. 2003a. Expression profile of the transient receptor potential (TRP) family in neutrophil granulocytes: Evidence for currents through long TRP channel 2 induced by ADP-ribose and NAD. Biochem J 371:1045–1053.

Heiner I, Eisfeld J, Luckhoff A. 2003b. Role and regulation of TRP channels in neutrophil granulocytes. Cell Calcium 33:533–540.

Iwata Y, Matanosaka Y, Arai Y, Komamura K, Miyatake K, Shigekawa MA. 2003. A novel mechanism of myocyte degeneration involving the Ca^{2+}-permeable growth factor-regulated channel. J Cell Biol 161(5):957–967.

Jahnel R, Bender O, Munter LM, Dreger M, Gillen C, Hucho F. 2003. Dual expression of mouse and rat VRL-1 in the dorsal root ganglion derived cell line F-11 and biochemical analysis of VRL-1 after heterologous expression. Eur J Biochem 270:4264–4271.

Jordt SE, Julius D. 2002. Molecular basis for species-specific sensitivity to "hot" chili peppers. Cell 108:421–430.

Kanzaki M, Zhang YQ, Mashima H, Li L, Shibata H, Kojima I. 1999. Translocation of a calcium-permeable cation channel induced by insulin-like growth factor-I. Nat Cell Biol 1:165–170.

Kedei N, Szabo T, Lile JD, Treanor JJ, Olah Z, Iadarola MJ, Blumberg PM. 2001. Analysis of the native quaternary structure of vanilloid receptor 1. J Biol Chem 276:28613–28619.

Liang Y, Tedder TF. 2001. Identification of a CD20-, FcepsilonRIbeta-, and HTm4-related gene family: Sixteen new MS4A family members expressed in human and mouse. Genomics 72:119–127.

Liang Y, Buckley TR, Tu L, Langdon SD, Tedder TF. 2001. Structural organization of the human MS4A gene cluster on chromosome 11q12. Immunogenetics 53:357–368.

MacKrill JJ. 1999. Protein–protein interactions in intracellular Ca^{2+}-release channel function. Biochem J 337: 345–361.

Mery L, Strauss B, Dufour JF, Krause KH, Hoth M. 2002. The PDZ-interacting domain of TRPC4 controls its localization and surface expression in HEK293 cells. J Cell Sci 115:3497–3508.

Minke B, Cook B. 2002. TRP channel proteins and signal transduction. Physiol Rev 82:429–472.

Muraki K, Iwata Y, Katanosaka Y, Ito T, Ohya S, Shigekawa M, Imaizumi Y. 2003. TRPV2 is a component

of osmotically sensitive cation channels in murine aortic myocytes. Circ Res 93:829–838.

Petrecca K, Atanasiu R, Akhavan A, Shrier A. 1999. N-linked glycosylation sites determine HERG channel surface membrane expression. J Physiol 515:41–48.

Stokes AJ, Shimoda LMN, Koblan_huberson M, Adra CN, Turner H. 2004. A TRPV2/PKA signaling module for transduction of thermal stimuli in mast cells. J Exp Med 200:137–147.

Tagoh H, Kishi H, Muraguchi A. 1996. Molecular cloning and characterization of a novel stromal cell-derived cDNA encoding a protein that facilitates gene activation of recombination activating gene (*RAG*)-1 in human lymphoid progenitors. Biochem Biophys Res Commun 221:744–749.

Trimmer JS. 2002. Unexpected cross talk: Small GTPase regulation of calcium channel trafficking. Sci STKE 2002:E2.

Turner H, Kinet JP. 1999. Signalling through the high-affinity IgE receptor Fc epsilonRI. Nature 402:B24–B30.